5

Diagnosis and Imaging of Corneal Astigmatism

Jaime Tejedor[1,2] and Antonio Guirao[3]
[1]*Hospital Ramón y Cajal,*
[2]*Universidad Autónoma de Madrid,*
[3]*Universidad de Murcia,*
Spain

1. Introduction

Accurate diagnosis and measurement of corneal astigmatism is of vital importance for treatment. Refractive and corneal astigmatic power and axis values are correlated but not coincidental. Corneal power and astigmatism amount measurements have a considerable degree of variability, which may be due to systematic error of the devices employed. Test to test variations may be falsely estimated as surgically induced refractive or astigmatic changes. Manual and automated keratometry instruments sometimes yield non-coincidental corneal power and axis readings, with differing reproducibility or repeatability. Even among modern automated keratometry, Placido-disk based videokeratoscopy and advanced slit-scanning or Scheimpflug technology scanning, diverging corneal measurements have been reported, which are attributable to different underlying methodology, reliability and repeatability.
In this chapter, we will summarize the basic functioning principles of the main devices used for the evaluation of corneal power and astigmatism. We will also review published studies about variations in corneal power measurements using different equipment, in astigmatic power and axis calculated values, and correlation obtained among measurements taken with different instruments. Results reported by different authors will be compared with our own data where available.

2. Keratometry

2.1 Principles of keratometry

A keratometer measures the radius of curvature of a small portion of the central cornea assuming it to be spherical, with constant radius of curvature, and radially symmetrical. Radius is calculated using geometric optics considering the cornea as a spherical reflecting surface (Horner et al, 1998), based on the fact that the front surface of the cornea acts as a convex mirror. The cornea is a high-powered mirror. With a constant distance between the eye and keratometer, the corneal radius is directly proportional to the size of the reflected image it produces (Purkinje I) and indirectly proportional to the size of the object (see Figure 1). To measure the size of the image relative to the object, the tiny image has to be magnified (American Academy of Ophthalmology [AAO], 2005). Because the eye is constantly moving, with 2 base to base prisms positioned so that the baseline splits the pupil, the observer sees two images separated by a fixed amount (Rabbetts, 1998). Any oscillation of the cornea will affect both images, and separation between them will not change (doubling principle). Therefore, the observer may arrive to the desired measurement position more easily.

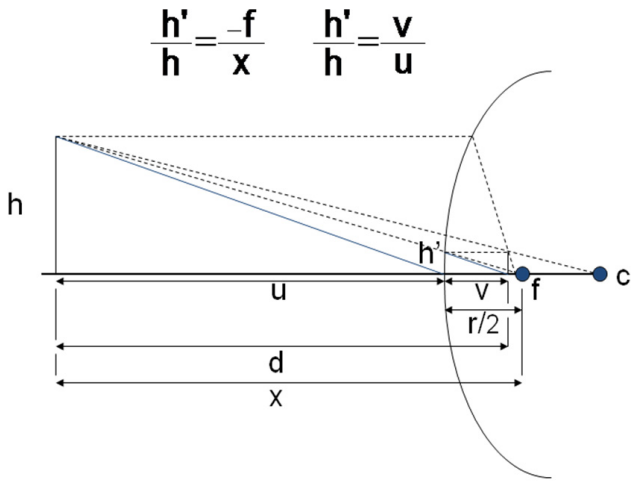

Fig. 1. Schematic diagram presented to illustrate the principles of keratometry. The cornea is a spherical reflecting surface or mirror. An illuminated object of known size or height (h) is placed at a known distance from the cornea. By similar triangles, the ratio of object height to distance (x, distance from mires to convex mirror focal plane, approximated by d, distance from the mires to the image) equals the ratio of image size (h') to focal distance (-f). The radius of curvature, which is twice the focal distance, is then calculated. u: distance from object to cornea; v: distance from cornea to image; c: center of curvature of the cornea.

Keratometers do not measure refractive power of the cornea. Measurements of radius of curvature, r (meters) can be converted to power, P (diopters) using the formula $P= (n_2-n_1)/r$, where n_1 is the refractive index of the first medium, and n_2, refractive index of the second medium. It applies to the anterior (air-cornea) and posterior (cornea-aqueous) corneal surface, but the curvature of the posterior corneal surface is not actually measured, estimating the total corneal power by a reduced refractive index, standard keratometric index (usually n= 1.3375), that takes into account the negative power of about -6.00 diopters of the corneal back surface (Corbett et al, 1999). Because the refractive index of air is $n_1= 1$, $P= 0.3375/r$. Helmholtz and other early designers of keratometers were interested in measuring the contribution of the cornea to the refractive power of the eye, as if the cornea was a lens with a single refracting surface. Theoretically, if one wishes to know the refractive power of only the anterior corneal surface, one must multiply the dioptric reading on the keratometer by a factor of 1.114 to correct for Helmholtz's fudge factor (Krachmer & Mannis, 2005). Javal and Schiötz chose 1.3375 as calibration index probably influenced by the fact that 7.5 mm corresponds exactly to 45 D (Haag-Streit), and that in normal corneas the posterior radius of curvature averages 1.2 mm less than that of the anterior surface. Several studies showed that this power overestimates the total power of the cornea by approximately 0.56 D. Other manufacturers adopted 1.332 or 1.336 as calibration index, which many authors consider the best choice because it is the accepted value for the refractive index of tears and the aqueous humor. The anterior radius of the cornea and a net index of refraction of 4/3 (1.333) is commonly used today to calculate the net power of the cornea. Using this lower value, the total power of a cornea with an anterior radius of 7.5 mm

would be 44.44 D. A useful rule of thumb is that a radius of difference of 0.2 mm indicates approximately 1 D of corneal astigmatism, for average radii and small amounts of astigmatism (Howes, 2009). For an estimation of only the front surface power of the cornea, a refractive index of 1.376 should be used, which is the true corneal index.
Calculations are based on the geometry of a spherical reflecting surface (Horner et al), although the cornea is described as prolate, flattening from center to periphery, and ellipsoid (i.e., true apical radius is steeper than measured, and steeper than the peripheral cornea). Quantitative data are based on only four points in the central 3 millimeters ring mire of the cornea in the standard keratometer, but different types of keratometer use differently sized mires at differing separations. Therefore, it provides gross qualitative indication of corneal regularity between them. Keratometry assumes paraxial optics, and is not valid when higher accuracy is required or peripheral areas have to be measured. When the cornea differs from a spherocylindrical surface lens, the keratometer does not measure it accurately.
Other limitations of keratometry are: (1) the assumption that the corneal apex, line of sight, and axis of the instrument coincide, which is not usually true, (2) the formula approximates the distance to focal point by the distance to image, (3) the power in diopters depends on an assumed index of refraction, and (4) the "One-position" instruments, in which it is possible to measure two orthogonal meridians without rotating the instrument, assume regular astigmatism (Horner et al, 1998).
Keratometers measure corneal astigmatism as the difference between the powers of the two principal meridians, and they have been the classical devices used to determine astigmatism of the cornea.

2.2 Types of keratometer

There are two main types of keratometer, manual and automated keratometers.

2.2.1 Representative models of manual keratometer

In the Javal-Schiötz keratometer (1880), the doubling is fixed and the separation of the mires is varied by moving them symmetrically round a circular path approximately concentric with the cornea under test (Rabbetts, 1998). In the traditional pattern, one the mires is red and the other green, and they have to be set in apposition to measure the flatter and steeper meridian (two-position keratometer), any overlap producing yellow. In off-axis position with respect to the cornea, the black central line of one mire image becomes out of alignment with its fellow on the other mire. Scissors distortion may also be apparent.
Another commonly used keratometer is the Bausch and Lomb keratometer (1932). Mire separation (object size) is fixed and doubling variable (image size measured). It is the typical one-position instrument in current use (Rabbetts, 1998). A lamp bulb illuminates the circular mire, and three images of the mire are seen in the eyepiece, a central one and two others doubled in mutually perpendicular directions. The central image appears slightly doubled unless in correct focus. Plus and minus signs surrounding the circular mires are used as measurement marks. When correct meridional alignment has been established, the two radius settings can be made in sequence by adjusting the doubling, when the adjacent plus and minus signs are brought into exact coincidence. There is a fixation point for the patient who sees a reflection of his own eye.
The range of measurement of the keratometer is frequently from 36.00 to 52.00 D, but in some cases it is very wide, from 28.00 to 60.00 D (Topcon OM-4).

2.2.2 Automated keratometers

The Humphrey autokeratometer measures corneal curvature by projecting three beams of near infrared light on to the cornea in a triangular pattern within an area about 3 mm in diameter. After reflection, they are received by directional photo-sensors which effectively isolate rays making a predetermined angle with the instrument's optical axis. This recalls a variable doubling keratometer in which the mires subtend a constant angle at the cornea. The source is a light-emitting diode (LED) and the ray paths are reversed. The precise location of the reflection point on the cornea is determined by the position of a rotating chopper which sweeps across all three beams and is imaged in the plane of the cornea by a projector lens. From the information provided by the three beams, the principal radii and meridians of the cornea can be calculated. At the start, the patient fixates a central red LED while the instrument is aligned by the operator and monitoring systems (Rabbetts, 1998).

Canon, Nidek, and Topcon have their respective auto-keratometers, usually combined with an auto-refractor. In Canon models an annular lens projects collimated light from a ring mire on to the cornea. The mire reflection is projected on to a detector system consisting of five sectors. From the light distribution on each of these sectors the computer is able to calculate the corneal radii. The diameter of the measuring zone is slightly larger than that of the Bausch and Lomb instrument. In the Topcon instrument, the observation system is telecentric, and a pinhole aperture restricts the rays reflected from the cornea to paths parallel to the instrument's axis (Rabbetts, 1998). Diameter of corneal zone measured varies among automated keratometers. For example, Nidek ARK510A uses 3.3 mm, whereas Humphrey ARK599 uses 3.0 mm. However the IOLMaster incorporated keratometer utilizes a 2.3 mm measurement diameter (Goggin et al, 2010).

The Scheiner principle is the basis of many automated refractors, which also give keratometry (MacInnis, 1994). Using a double aperture system, when the object of regard is placed conjugate to the retina a single clear image is formed. Under a condition of ametropia, the image is double, and can be converted to a single image with an optometer. This can be done by focusing visible or infrared light on the retina, and different meridians could be measured to determine astigmatism.

3. Computerized corneal topography

Corneal power and astigmatism may be measured also using computerized devices. Methods for measuring corneal topography fall into two broad categories: reflection-based and projection-based methods.

3.1 Reflection-based methods

Videokeratoscopy arose from the desire of investigators to quantitate the corneal shape information available in keratoscope images. Keratoscopes were designed more than 100 years ago, when investigators realized that the diseased cornea could have a curvature that differed significantly from a spherocylindrical lens. The keratoscopes project an illuminated target, more complex than that of keratometers, to generate an image reflected by the corneal surface. Reflection-based methods commonly take the form of Placido-disk type concentric rings. The images of multiple reflected luminous concentric circles projected on the corneal surface are digitally analyzed. Therefore, curvature of the posterior cornea is not actually measured. The position of each point to be measured on the many circle mires from the center to the periphery of the cornea should be determined first. Most systems measure

between 256 and 360 points around the circumference of each mire, but leave unmeasured the areas between the mires (Krachmer & Mannis, 2005). Videokeratoscopes commonly use a polar coordinate system to identify a specific corneal position relative to the center of the image, at a distance from the center and at a defined angular position. The image is two-dimensional, and doesn't provide information on changes in corneal elevation.

When axial measurements are taken (Corbett et al, 1999), these units assume the angle of incidence to be nearly perpendicular, and the radius of curvature to be the distance from the corneal surface to the intersection with the visual axis or line of sight of the patient (axial distance). The slope of a curved surface is the gradient of the tangent at a particular point (first differential of a curve). Slope could be referred to as the angle (θ) between the tangent vector of the curve at that point and the x unit vector or center corneal axis. It is converted to radius of curvature by the equation $r = d/\cos\theta$, where d is the distance from the point on the corneal surface to the axis. Curvature is given by $\kappa = d\theta/ds$, where s is the arclength parameter, and amounts to $\kappa = |y''|/ [1 + (y')^2]^{3/2}$. Axial maps curvature values approximate the power of the central 2-4 mm of the cornea, where sphericity may be assumed. From these values, an iterative process algorithm is used, making a series of assumptions, to describe the shape and power of the peripheral cornea with less accuracy, because elevation of a point in the z-axis cannot be determined directly by reflection-based methods. Variable degrees of surface smoothing are incorporated in the algorithms. The only position on the surface at which axial measurements are an accurate reflection of local refractive power is in the paraxial portion of the cornea. Normal corneas show decreasing power toward the periphery as displayed by the Placido-disk based topographers, which intuitively indicates the normal flattening of the cornea, but does not represent the true refractive powers. Based on Snell's law, the corneal power must increase in the periphery, due to the increasing angle of incidence, in order to refract the light into the pupil (spherical aberration).

In tangential maps, the instantaneous radius of curvature is calculated at a certain point (Horner et al, 1998; Corbett et al, 1999). The radius corresponds to the sphere with the same curvature at that point, determined by taking a perpendicular path through the point in question, in a plane that intersects the point and the visual axis, but not based on distance to the axis. Stated another way, local radius of curvature is calculated at each point with respect to its neighbouring points by estimation of the best-fit sphere, without reference to the visual axis or the overall shape of the cornea. There is greater accuracy in the periphery of the cornea and in representing local changes. Tangential maps show less smoothing of the curvature than axial maps.

The maps described attempt to depict the underlying shape of the cornea by scaling curvature through the familiar dioptric notation instead of radius millimeters, and powers are then mapped using standard colors to represent diopter changes. Diopters are relative units of curvature but not the equivalent of diopters of corneal power (Figure 2).

To represent shape directly, maps may display a z height from an arbitrary plane (iris, limbus, best-fit or reference sphere), plotted to show differences but not directly clinically important data, although the z values are frequently used to derive radius of curvature at that point.

3.2 Projection-based methods

In projection-based methods, an image is formed on the cornea, frequently using a slit beam scan, but sometimes by a grid pattern, Moiré interference fringes, or laser interferometry. Height or elevation data measurements above a reference plane are immediately available

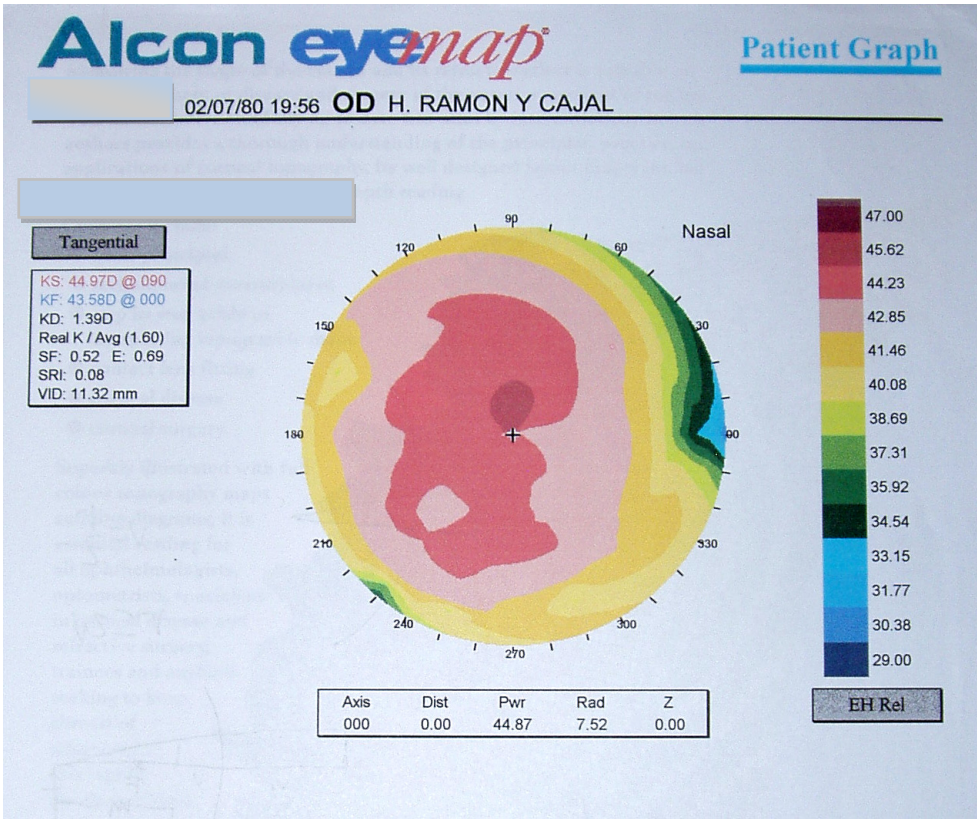

Fig. 2. Reflection-based system videokeratography. Using Alcon Eye Map EH-290, 1.4 D of corneal astigmatism, with an ellipsoid-bow tie intermediate pattern color map, is depicted.

from these systems (Corbett et al, 1999). Slope and curvature data can be calculated directly. Axial and tangential maps can also be obtained using these devices. These systems provide a more sensitive measure of variation in contour across the corneal surface, particularly in terms of slope and curvature. Refractive power measures derived are less accurate, due to the assumptions and approximations made during its calculation.

In slit-scanning systems, the machines project a series of slit beams at closely spaced intervals across the cornea. The computer software identifies the location of the anterior and posterior corneal margins of each individual slit section, and by smoothing digitized information, infers the shape and corneal thickness (Krachmer & Mannis, 2005). The resultant smoothed data in the Orbscan, a commercially available instrument that performs these functions, include anterior corneal curvature, posterior corneal curvature, and regional differences in corneal thickness between them. A color coding scheme is used for anterior corneal curvature, posterior corneal curvature and regional pachymetry maps. Output artifact under certain situations like opacities of the stroma, or inaccurate digitizing of the posterior corneal surface, anterior to the real posterior cornea, when measuring post-LASIK corneas, may occur.

A rotating Scheimpflug camera generates Scheimpflug images in three dimensions in Pentacam and Galilei systems. In no more than 2 seconds a complete image of the anterior segment is generated. Any eye movement may be detected by a second camera and corrected for in the process. Scheimpflug images are digitalized and transferred, and a 3D virtual model of the anterior eye segment is calculated. Anterior and posterior cornea elevation and curvature data are thus obtained. Corneal thickness is consequently derived.
High-frequency ultrasound and optical coherence tomography are techniques for corneal imaging, at an early stage of development for three-dimensional reconstruction of the cornea.

4. Definitions for the evaluation of corneal measurement devices

Accuracy refers to the degree of closeness of measurements of a quantity to its actual (true) value (validity). In accurate measurements the systematic error is small.
Precision of a measurement system, including repeatability and reproducibility, is the degree to which repeated measurements under unchanged conditions show the same results (reliability). Measurements are precise when the random error is small. Repeatability is usually considered as the variability of the measurements obtained by one same person (intraobserver) while measuring the same item repeatedly, under the same conditions and over a short period of time. When two measurements are taken using the same device, coefficient of repeatability may be calculated as COR= 1.96 x Standard Deviation (of difference between the two measurements). Reproducibility is the variability of the measurement system caused by differences in operator behavior, or variability of the average values obtained by several operators (interobserver) while measuring the same item.

5. Evaluation of the cornea using keratometry

Keratometry may be used not only to estimate the dioptric curvature of the anterior ("total") cornea and infer astigmatism but also to evaluate the quality of the corneal surface. In the presence of pathology in the central visual axis, keratometric mires would be irregular. Every time readings are taken, the quality of the mires should be described as regular, when they overlap perfectly, or mildly to markedly irregular, when they do not overlap perfectly (Krachmer & Mannis, 2005). These patterns may help to predict best-corrected visual acuity, because the examiner can judge with some certainty the visual potential from the anterior corneal surface abnormalities. In patients with keratoconus, inferior corneal steepening is easily observed by taking readings with the patient looking straight ahead and subsequently looking up slowly. Inferior steepening is present when the vertical mires slowly spread apart and get smaller. For most normal corneas, keratometry is sufficiently accurate for contact lens fitting and intraocular lens power calculation.
An important limitation of keratometry is the measurement of the cornea following LASIK or PRK procedures. The measurements are not accurate because the assumed net index of refraction is no longer appropriate for the new relationship of the front and back radius of the cornea. Following keratorefractive surgery, the assumptions that the central cornea may be approximated by a sphere and that the radius of curvature of the posterior cornea is 1.2 mm less than that of the anterior cornea, are no longer true (Howes, 2009). Automated keratometers which sample a smaller central area of the cornea (about 2.6 mm) relative to

manual keratometers, provide more accurate values of the front radius of the cornea, because the transition areas are far outside the zone that is measured. However, measures of the cornea are still not accurate. Automated and manual keratometers overestimate the power of the cornea proportionately to the amount of LASIK or PRK performed (by approximately 14%).

The accuracy and precision of keratometry depends largely on the care with which the instrument to cornea distance is adjusted, which requires accurate focusing of the eyepiece upon its graticule, especially in manual keratometers, and alignment of the instrument with the patient's eye. The latter is not always easy due to the small field of view, and isolated areas of the objective aperture, in instruments with doubling systems, with an exit pupil of possibly 3 mm overall diameter. The instrument utilizes small reflected areas no less than 1 mm and up to 1.7 mm from the center (Rabbetts, 1998). Because of the peripheral flattening, keratometer readings are slightly longer than the vertex radius. The error would probably not exceed 0.05 mm on a normal eye. A local distortion of the cornea in the region of the reflection areas will cause a corresponding distortion of the mires and uncertain focusing. Since the image is formed by reflection from the tear layer, variations in it may affect the quality and size of the image. The limits set by diffraction on the accuracy of keratometers indicate that the limit on repeatability could be no lower than 0.2 D, corresponding to a spread of about 0.04 mm on average radii. Reported accuracy of the Bausch and Lomb keratometer measurements vary from ± 0.25 D to ± 0.93 D (Rabbetts, 1998).

Repeatability of corneal power measurements with keratometer is good, but with different levels of precision depending on the study. Mean difference between the measured and actual surface power using Bausch and Lomb keratometer (Karabatsas et al, 1998) in four steel balls (2.7 mm to 3.4 mm radius of curvature) was -0.11 D (SD 0.09). Karabatsas et al found a coefficient of repeatability for intraobserver measurements of 0.22 D for steep meridian power and 0.18 D for flat meridian power, using 10 SL/O Zeiss keratometer. For steep and flat meridian axis, COR was 5° to 8°, and for astigmatism COR was between 0.20 D and 0.26 D, with the same device. Interobserver COR for steep axis power was 0.24 D, and for flat axis power was 0.20 D. For steep and flat meridian axis COR was 8°, and for astigmatism, COR was 0.28 D. In postkeratoplasty corneas, COR was greater than in normal corneas, but better than using topographic maps.

Elliott et al reported (Elliott et al, 1998) that Bausch and Lomb manual keratometer showed poorer repeatability than automated keratometry devices (Nikon NRK-8000 and Nidek KM-800). Coefficient of repeatability values for the vertical, torsional, and horizontal meridians were 0.55 D, 0.42 D and 0.70 D, respectively, for the B&L keratometer. However, the Nikon coefficients of repeatability for the same meridians were, respectively, 0.34 D, 0.23 D, and 0.27 D, whereas the Nidek values were, respectively, 0.34 D, 0.18 D, and 0.32 D. The same conclusion is reached by Shirayama et al, who measured repeatability as coefficient of variation (ratio of the SD of the repeated measurements to the mean in %), to study B&L manual keratometer and IOL Master, in addition to different topographer devices (Shirayama et al, 2009). IOL Master showed a CV of 0.09 (±0.07) and B&L manual keratometer showed a CV of 0.18 (±0.12). However, Intraclass correlation (ICC) was high with the two devices (0.99 in both keratometers). In this study, automated keratometry had also higher repeatability than Galilei Dual Scheimpflug analyzer and Humphrey Atlas Corneal Topographer. These devices had CV of 0.12 (±0.07) and 0.22 (±0.12), respectively, with B&L manual keratometry in an intermediate position between the two. ICC of the

corneal topographer devices was similar to that showed by keratometers (0.99). When results of power measurements were compared between the four devices, all devices were significantly correlated with each other (Pearson correlation coefficient= 0.99 in all pairs).

6. Use of topographic maps in the evaluation of the cornea

The videokeratoscopy image may be examined in a specific fashion to detect alterations of normal concentric pattern, checking for artifacts (Maguire, 2005) when total and astigmatic corneal power is obtained. Focal tear film abnormalities appear as localized mire distortions, which may be caused by epithelial irregularity, mucus in the tear film, or exaggerated tear meniscus in the upper or lower lid. Central mires may be inspected to detect evidence of irregular astigmatism. Irregular astigmatism causes the mire to have an egg shape, or some other shape that differs from the circular or the elliptical shape corresponding to a cornea that approximates a spherocylindrical lens. When the space between adjacent mires reduces from the central to the peripheral cornea, the cornea is steepening, whereas wider spacing indicates relative flattening.

Placido disc or reflection-based topography units do not have the ability to measure the central 1.8 to 2.0 mm of cornea, and this information is currently extrapolated from the smallest reflected ring. This information from the central cornea is most important, since this is the crucial pathway for light through the pupil. Photoreceptor alignment weighs this central light more importantly, thus accounting for the Stiles-Crawford effect. Increasingly important is the ability to precisely measure the posterior cornea as opposed to their merely relying on the assumed relationship that exists between the anterior and posterior surfaces, as occurs in reflection-based systems, when only effective measures of the anterior cornea are obtained. This relationship does not hold constant when a corneal injury or keratorefractive surgery alters the anterior corneal curvature only. As a result, our estimation of overall or true corneal power includes potential error in these eyes, as previously described for keratometry. This is considered the predominant source of error when trying to calculate IOL power in patients who have undergone previous corneal refractive surgery.

A problem reported soon in the development of Placido-based systems was the susceptibility to errors in alignment and focusing. A small error of alignment or focusing in a test sphere (0.2 mm) can cause a fairly significant change in the measurement (Horner et al, 1998). Vertical misalignment can cause asymmetry that might be mistaken as early keratoconus. Where the videokeratoscope axis intersects the cornea with respect to the references of the eye remains a challenge. The geometric center of the cornea (anatomic center equidistant from opposite limbuses) or corneal apex (point of greatest sagittal height, z) may be a useful reference for contact lens design, but from an optical point of view, the pupillary axis (line from the center of the entrance pupil perpendicular to the corneal surface), line of sight (straight line from the fixation point to the center of the entrance pupil), or visual axis (ray from the fixation point that passes undeviated, through the nodal points, to the fovea), could be used as reference for these instruments. Mandell suggested the point where the line of sight intersects the cornea as a useful reference, whereas the visual axis, and its corneal intercept, is difficult to locate objectively (Mandell & Horner, 1993). However, when alignment of the instrument is implemented by manual or automated means, the axis of the videokeratograph becomes normal to the cornea, and passes through the center of curvature of the cornea and the coaxially sighted reflex centre, i.e., the site of

the corneal light reflex when the cornea is viewed coaxially with the light source. This point is nasally displaced, but considered to be closer to the corneal intercept of the visual axis than to the corneal intercept of the line of sight. Mandell examined this issue in detail (Mandell, 1994). In no case was the corneal intercept of the line of sight on the instrument axis, and infrequently the apex position was on the videokeratograph axis.

Another cause of spurious topography is irregularities in the tear film, particularly in reflection-based systems, because videokeratoscopes image the air-tear interface, and not exactly the corneal epithelium (Corbett et al, 1999). Pooling of tears in the lower meniscus produces a focal steepening, and thinning of the tear film by drying shows a localized flattening of the surface. Poor tear quality can interfere with the accuracy of the measurements in different ways, but some of these artifacts can be overcome by asking the patient to blink immediately before the image is captured.

Color-coded maps were initially developed for videokeratoscopy (Corbett et al, 1999). The warmer colors (red, orange, yellow) represented the steeper areas, whereas the cooler colors (green, blue) marked the flatter zones. A similar color-coded scale was applied to height maps with the introduction of projection-based systems, in which the high areas were depicted by warm colors, and the low areas by cool colors.

It is important to check the type of scale on the map under study. The label on the scale gives the type of measurement being displayed: height (mm or μm), slope (adimensional or mm/mm), curvature (mm), or power (diopters). The first step before studying the map is to check the number of steps, interval between the steps, and the range covered by the scale. Many systems enable the user to choose between a standardized absolute scale, in which there is a fixed color-coding, that is, the same colors always represent the same curvatures or powers, and the same for all subjects, and a normalized relative scale, in which the number of colors are automatically adjusted to the range of diopter values in that single map. In an adjustable scale map, the operator may select the step interval and diopter range of the contour (Corbett et al, 1999).

Height, curvature or power data can be presented as a plot of difference from a flat reference plane, a sphere of known size or an idealized corneal shape. Different commercial systems give indices of different names, which summarize a particular feature of the cornea. These include simulated keratometry (equivalent but not similar to measurements of keratometer), asphericity, surface asymmetry index (difference in corneal power between points 180° apart in the same ring), inferior-superior value (difference between superior and inferior points 3 mm from the center), surface regularity index (local regularity of the corneal surface in the central 4.5 mm diameter), index of surface variance (deviation of individual corneal radii from the mean value), index of vertical asymmetry (degree of symmetry of corneal radii with respect to the horizontal meridian). Some of these indices correlate with visual function or potential visual acuity. A keratoconus index is also presented by different systems. Using information from this and other indices, and additional clinical data, an index of suspicion of keratoconus or keratoconus level classification may be obtained. Anterior and posterior surface elevation data shown by slit-scanning or Scheimpflug photography systems also help diagnose keratoconus (typically, differences greater than +15 μm for anterior elevation indicate keratoconus).

Some authors have classified the topography of normal corneas according to the shape of the contour corresponding to the middle of the scale, in five patterns: round, oval, symmetric bow tie, asymmetric bow tie, and irregular (Bogan et al, 1990). The videokeratoscopic representation of corneal regular astigmatism (toric surface) has the

appearance of a bow tie, with the bows of the tie aligned along the steeper meridian. This pattern may occur in projection based systems (Figure 3) but, because they measure corneal height, commonly depict a toric surface as a series of concentric ellipses with their long axis in the flatter meridian (Corbett et al, 1999). When a best fit sphere is subtracted from the corneal height data, astigmatism shows as a ridge.

Bogan found a bow pattern in 49% of "normal" patients studied, and they had astigmatism much more frequently, particularly those with symmetric bow ties. In patients with bow patterns but no astigmatism, either the central portion of the cornea is spherical or corneal toricity is compensated by inverse lenticular astigmatism. An asymmetric bow tie represents asymmetry in the rate of change of the radius of curvature from center to periphery. This pattern is obtained sometimes in normal eyes with astigmatism, or in cases of contact lens warpage, early keratoconus, or artifact by poor fixation or decentration. An irregular pattern may also be the result of bad fixation, improper focusing or tear film abnormalities.

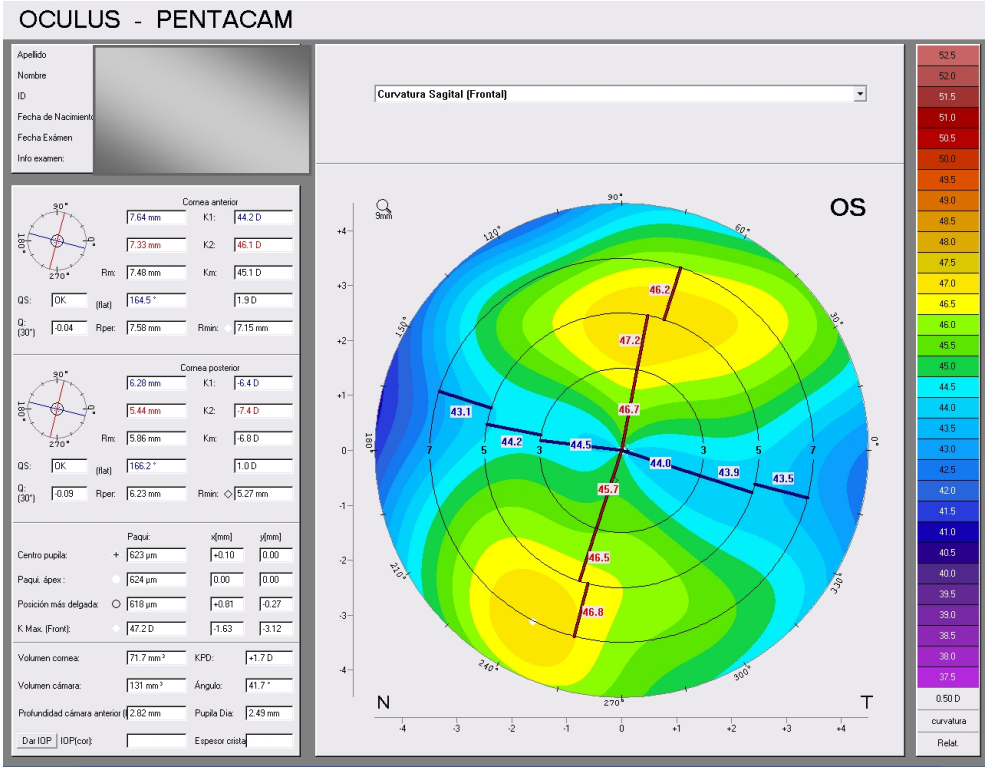

Fig. 3. Scheimpflug eye scanner analysis system image of the cornea. This figure illustrates 1.9 D of anterior corneal astigmatism with a bow-tie pattern.

In contact-lens induced corneal warpage, contact lens wear alters the shape of the cornea as a result of mechanical pressure or metabolic factors. Some patients are asymptomatic, others lose several lines of spectacle corrected visual acuity while maintaining good contact lens acuity, or develop contact lens intolerance. Many topographic patterns may result, including

irregular astigmatism, change in the axis of astigmatism, asymmetry, but most commonly flattening in the areas of lens bearing and relative adjacent steepening. Frequently, these changes can only be detected by computer-assisted videokeratography.

In reports of early topographers, CMS (Corneal Modeling System) was compared with Bausch and Lomb keratometer while measuring spherical surfaces (Hannush et al, 1989). No significant difference was found between the keratometer and the CMS in either accuracy or precision. Most of the rings in the videokeratograph were within ± 0.25 D of the known curvatures. Using a CMS with 31 rings (Computed Anatomy), mean difference of measured and actual surface power in four steel test balls (2.7 mm to 3.4 mm radius of curvature) was 0.10 D (SD 0.07D). Rings 2 through 26 were read accurately and precisely within ± 0.25 D on three of the four balls. On the steepest ball, values were within ± 0.37 D. In projection (Placido-disk) based videokeratography, repeatability of corneal measurements was frequently inferior to that of keratometry. Intraobserver COR for TMS was 0.3 D for steep meridian power and 0.44 for flat meridian power (Karabatsas et al, 1998). For astigmatism, it was 0.40 D, 22°-26° for steep meridian location, and 13°-30° for flat meridian location. Repeatability of the TMS was found to be observer related and astigmatism related. Interobserver COR was 0.92 D for the steep meridian power, 1.82 for the flat meridian power, and 1.26 D for astigmatism. Regarding axis meridian, interobserver COR was 40° for the steep axis, and 42° for the flat axis. A novice observer was found to have greater COR when compared with an experienced examiner. Higher deviation scores were also observed for corneas with higher astigmatism. In postkeratoplasty corneas, TMS achieved inferior repeatability and reproducibility than keratometry.

Heath et al (1991) concluded that the accuracy of CMS depended on the shape of the surface. For spheres, torics, and aspheric surfaces, 96.9%, 87.5%, and 60.4%, of measurements, respectively, were within ± 0.375 D. The measurements were highly repeatable, with a standard error of 0.02 D for 16 repeated measures.

The TMS-1 and EyeSys (Placido-disk based systems) were compared by Wilson et al (1992) using spherical surfaces and normal human corneas, and by Antalis et al (1993) using abnormal corneas. The two systems gave similar results, except for a small advantage using the TMS-1 with abnormal corneas. The TMS-1 was slightly more repeatable in the central 0.6 mm than the EyeSys was, according to Maguire et al (1993).

Applegate & Howland (1995) examined the accuracy of the TMS-1 in measuring "true surface topography", using elevation data from the instrument referenced to a plane perpendicular to the videokeratoscope axis, or calculating the elevation by integrating the slope of each sample point. Both methods yielded similar results on spheres, ellipses, and bicurves, with root mean square errors under 5 μm. The elevation found directly from the TMS-1 data files had larger errors, particularly on ellipses. For bicurves, the TMS-1 elevation files had lower errors, on the order of those found on ellipses, whereas calculated elevation had greater error. Surfaces with sharp transitions are not measured accurately, whereas in smooth elliptical surfaces calculating axial curvature yields better results than the elevation files. The error in the elevation files increases toward the periphery (Cohen et al, 1995; Mandell and Horner, 1993). Tomey TMS-2N system provides more reliable elevation files.

Davis and Dresner (1991) compared the accuracy of the EH-270 Alcon system with that of conventional keratometry and found the keratometer to be more accurate on four test spheres. The error increased as the test spheres became steeper. Younes et al (1995) examined the repeatability and reproducibility of Alcon EH-270 taking three measures of both eyes in 39 subjects. Initial repeated measures yielded standard deviations of 0.5 D on

the central 3 mm region and increased toward the periphery. Six months later, the differences did not exceed 0.375 D, and the corneal curvatures were found to be slightly steeper toward the center and slightly flatter toward the mid-periphery.

Roberts (1996) compared the accuracy of instantaneous curve algorithms for the Alcon EyeMap, TMS-1, EyeSys Corneal Analysis System, and Keratron on smooth aspheric surfaces. The results showed each of the systems to have approximately the same level of error.

More recently introduced topographers that use scanning slit of the cornea (Orbscan II), Scheimpflug photography images to derive keratometry data of the surface (Pentacam), or double Scheimpflug system combined with a Placido disk (Galilei analyzer) have also been evaluated. A study of curvature readings of the Galilei analyzer and Orbscan II systems demonstrated high intraclass correlation for flat and steep axes keratometry readings in Galilei (0.97 and 0.84, respectively) and Orbscan II (0.96 and 0.95, respectively), which indicates that variation in measurements reported was mainly due to subject-to-subject variation rather than error (Shirayama et al, 2009). The Galilei system provided somewhat flatter K values than the Orbscan II system. However, coefficient of repeatability for the measurements was not reported. Repeated keratometry measurements by the same or a different examiner showed virtually no intraobserver or interobserver variation error (0 to 0.3 D for both devices).The regression coefficient between Orbscan II and Galilei measurements was 0.79, and astigmatism values did not differ significantly between the two.

In a study using the 4-mm zone in Pentacam Scheimpflug technology, reproducibility of two different measures of the cornea taken 1 month apart had an average difference of 0.37 D, with a maximum difference of 0.50 D (Shankar et al, 2008). Pentacam measures the true corneal power in postoperative LASIK and PRK patients to an accuracy of ±0.50D. According to Shankar et al., Pentacam corneal curvature measurements show excellent repeatability. We tested repeatability of Pentacam eye scanner in nine patients, with two measurements in each patient, 5 minutes apart. Intraclass correlation was 0.98, with a standard deviation of difference between mean K measurements of 0.14 D (0.09–0.36).

Because test to test variations occur in corneal measurements, a value could be derived from one test to the next, which has been termed astigmatism measurement variability. It would be similar to calculation of surgical change in astigmatic values, termed surgically induced astigmatism, but without surgical intervention. In a recent study, 4 keratometric devices were used to examine astigmatism measurement variability, and to determine which was most reliable, and which produced the least bias, including Nidek ARK510A, Humphrey ARK599, IOLMaster V3.02, and Pentacam HR7900 (Goggin et al, 2010). Intraclass correlation for flat and steep K keratometric measurements, and for the meridian of the steep K for each eye, were all greater or equal to 0.93, except for Pentacam steep meridian, which was 0.85. Nidek had particularly high ICC for the 3 measurements, as was IOLMaster, except for steep K meridian which was somewhat lower in IOLMaster. Nidek was the most precise of the 3 devices, as indicated by lower CV values than the other instruments.

Nidek, Humphrey, and IOLMaster produced similar astigmatism measurement variability values (0.24 ± 0.2 D, 0.22 ± 0.13 D, and 0.28 ± 0.25 D, respectively), but Pentacam produced a significantly larger value (0.46 ± 0.46 D, p= 0.01). The vector means for the astigmatism measurement variability were small, but larger for and IOLMaster and Pentacam (Nidek, 0.03 D x 41°; Humphrey, 0.08 D x 12°; Pentacam, 0.14 D x 115°; IOLMaster, 0.10 D x 142°), whereas Nidek had the lowest value. Nidek ARK510A is more reliable than the other 3

devices. All studied devices demonstrated a clinically significant astigmatism measurement variation (0.22 to 0.46 D), which means that a significant proportion of keratometric surgically induced astigmatism reported in the literature may be due to variation in keratometric measurement.

According to our data, obtained in 32 patients measured twice (5 minutes apart measurements) using three devices similar to the previous study (Pentacam, IOLMaster, Nidek ARK510) and a manual keratometer (Topcon OM-4 ophthalmometer), the coefficient of repeatability was better for the steep K measurement than for the flat K measurement in all devices except IOLMaster. IOLMaster and Nidek had the best repeatability for K values, but IOLMaster had the lowest COR values (0.1 D for flat and 0.3 D for steep keratometry values). Shankar et al obtained a COR of 0.28 D for mean keratometry in Pentacam anterior corneal measurements, similar to our findings, whereas our COR obtained for steep K was 0.6 D using this instrument for anterior corneal surface. The lowest COR for the flat axis measurement was that of Nidek (24°). Regarding astigmatic cylinder, the lowest COR was again for IOLMaster (0.33 D), followed by Nidek (0.62 D). Figure 4 depicts Bland-Altman 95% confidence interval limits of agreement for flat K values obtained with the IOLMaster.

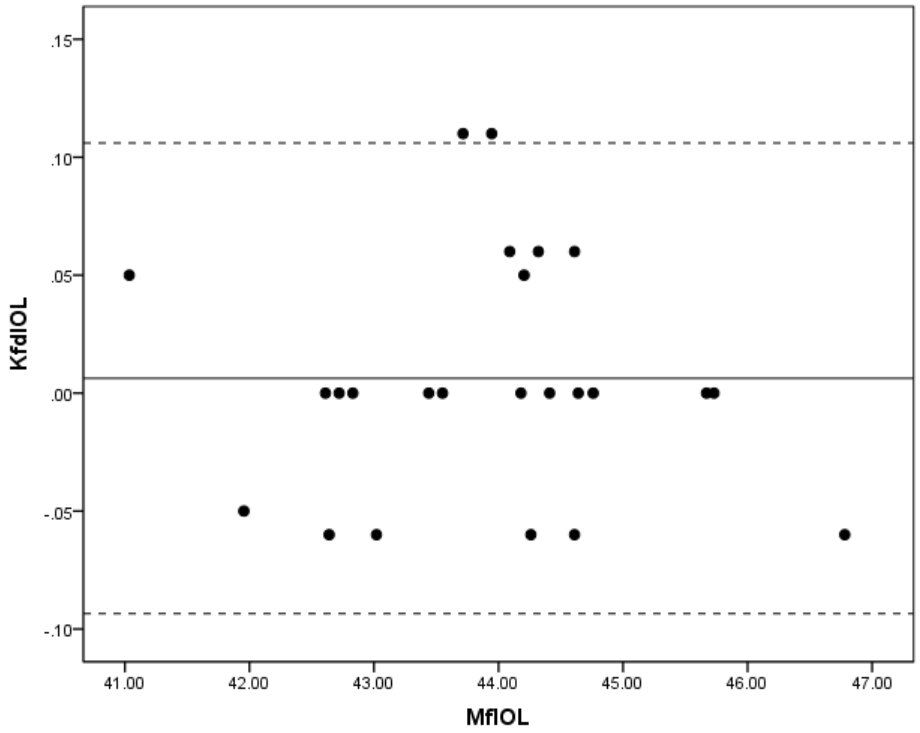

Fig. 4**.** Repeatability of IOLMaster automated keratometry readings. Bland-Altman analysis showing 95% confidence interval limits of agreement of difference between two measurements of the flat K readings (KfdIOL) versus mean flat K measurements (MfIOL), using IOLMaster technology.

Intraclass correlation was high for K values, flat axis, and astigmatism. ICC for steep and flat K values was 0.99 and 0.97 in Nidek, 0.99 and 0.99 for IOLMaster, 0.98 and 0.82 in OM-4, and 0.96 and 0.88 for Pentacam, respectively. ICC for the flat axis was 0.98 for Nidek, 0.91 for IOLMaster, 0.72 for OM-4, and 0.92 for Pentacam. ICC for astigmatic cylinder was 0.86 for Nidek, 0.98 for IOLMaster, 0.90 for OM-4, and 0.3 for Pentacam anterior corneal surface.

7. Conclusions

Focusing and alignment are very important issues in the use of keratometers and corneal topographers to determine K diopter values and astigmatism. Automated keratometers have higher repeatability than manual keratometers and topographers. Corneal topographers can provide direct measurements of height and corneal periphery, but their main limitation for the moment is repeatability.

8. References

American Academy of Ophthalmology. (2005). Chapter 9: Telescopes and Optical instruments, In: *Clinical Optics*, American Academy of Ophthalmology, pp. 269-324, 1-56055-501-7, San Francisco.

Antalis J, Lembach R, Carney L. (1993). A comparison of the TMS-1 and the corneal analysis system for the evaluation of abnormal corneas. *CLAO J* 19 (1), pp. 58-63.

Applegate R, Howland H. (1995). Noninvasive measurement of corneal topography. *IEEE Eng Med Biol* 14 (1), pp. 30-42.

Bogan SJ, Waring GO, Ibrahim O, Drews C, Curtis L. (1990). Classification of normal corneal topography based on computer-assisted videokeratography. *Arch Ophthalmol* 108 (), pp. 945-949.

Cohen KL, Tripoli NK, Holmgren DE. (1995). Assessment of the power and height of radial spheres reported by a computer-assisted keratoscope. *Am J Ophthalmol* 119 (6), pp. 723-732.

Corbett MC. (1999). *Corneal Topography: Principles and applications*, BMJ Books, 0-7279-1068-X, London.

Davis L, Dresner M. (1991). A comparison of the EH-270 corneal topographer with conventional keratometry. *CLAO J* 17 (3), pp. 191-196.

Elliott M, Simpson T, Richter D, & Desmond F. (1998). Repeatability and comparability of automated keratometry: the Nikon NRK-800, the Nidek KM-800 and the Bausch and Lomb keratometer. *Ophthal Physiol Opt* 18 (3), pp. 285-293.

Goggin M, Patel I, Billing K, & Esterman A. (2010). Variation in surgically induced astigmatism estimation due to test-to-test variations in keratometry. *J Cataract Refract Surg* 36 (10), pp. 1792-1793.

Hannush SB. (1989). Accuracy and Precision of Keratometry, Photokeratoscopy, and Corneal Modeling on Calibrated Steel Balls. *Arch Ophthalmol* 107 (8), pp. 1235-1239.

Heath G, Gerstman D, Wheeler W. (1991). Reliability and validity of videokeratoscopic measurements. *Optom Vis Sci* 68 (12), pp. 946-949.

Horner DG, Salmon TO, & Soni PS. (1998). Chapter 17: Corneal Topography, In: *Borish's Clinical Refraction*, William J Benjamin, ed, pp. 524-558, WB Saunders Company, 0-7216-5688-9, Philadelphia.

Howes FW. (2009). Chapter 5.3: Patient work-up for cataract surgery. In: *Ophthalmology*, 3rd ed, Yanoff M, Duker JS, eds, pp. 410-422. Elsevier Mosby, 978-0-323-04332-8, Philadelphia.

Karabatsas CH, Cook SD, Papaefthymiou J, Turner P, & Sparrow JM. (1998). Clinical evaluation of keratometry and computerized videokeratography: intraobserver and interobserver variability on normal and astigmatic corneas. *Br J Ophthalmol* 82 (3), pp. 637-642.

Krachmer JH, Mannis MJ. (2005). Chapter 11: Refraction of the abnormal cornea, In: *Cornea*, 2nd ed, Volume 1. Krachmer JH, Mannis MJ, Holland EJ, eds, pp. 167-170, Elsevier Mosby, 0 323 03215 0, Philadelphia.

MacInnis BJ. (1994). Chapter 15: Instruments. In: *Optics & Refraction*, Brent J McInnis, ed, pp. 156-172, Mosby, 0-8016-7999-0, St Louis.

Maguire L, Wilson S, Camp J. (1993). Evaluating the reproducibility of topography systems on spherical surfaces. *Arch Ophthalmol* 111 (2), pp. 259-262.

Maguire LJ. (2005). Chapter 12: Keratometry, Photokeratoscopy, and Computer-assisted topographic analysis. In: *Cornea*, 2nd ed, Volume 1. Krachmer JH, Mannis MJ, Holland EJ, eds, pp. 171-184, Elsevier Mosby, 0 323 03215 0, Philadelphia.

Mandell R. (1994). Apparent pupil displacement in videokeratography. *CLAO J* 20 (2), pp. 123-127.

Mandell R, Horner D. (1993). Alignment of videokeratoscopes. In: *An Atlas of Corneal Topography*, Sanders D, Cock D, eds, pp. 197-204, Slack Inc, Thorofare.

Rabbetts RB. (1998). Chapter 20: Measurement of ocular dimensions, In: *Bennett & Rabbetts Clinical Visual Optics*, Ronald B Rabbetts, ed, pp. 378-405, Butterworth-Heinemann, 0-7506-1817-5, Oxford.

Roberts C. (1996). Accuracy of instantaneous radius of curvature algorithms in four Placido-ring based corneal topography devices using surfaces with aspheric profiles. Invest Ophthalmol Vis Sci 37 (3), Abstract 2558.

Shankar H, Taranath D, Santhirathelagan CH, Pesudovs K. (2008). Anterior segment biometry with the Pentacam: Comprehensive assessment of repeatability of automated measurements. J Cataract Refract Surg 34 (), pp. 103-113.

Shirayama M, Wang L, Weikert MP, Koch DD. (2009). Comparison of corneal powers obtained from 4 different devices. *Am J Ophthalmol* 148 (4), pp. 528-535.

Wilson S, Verity S, Conger D. (1992). Accuracy and precision of the corneal analysis system and the topographic modeling system. *Cornea* 11 (1), pp. 28-35.

Younes M, Boltz R, Leach N. (1995). Short and long-term repeatability of Visioptic Alcon EyeMap (Visioptic EH-270) Corneal Topographer on normal human corneas. *Optom Vis Sci* 72 (11), pp. 838-844.